

9.3 Non-null Test

Can use geometrical tests such as Foucault, wire, or Ronchi tests, but we will only discuss interferometric tests. One advantage of interferometric tests is that they are fairly easy to computerize.

9.3.1 Lateral shear interferometry

- Advantages

Can vary the sensitivity by varying the amount of shear.

- Disadvantages

Two interferograms are required for non-rotationally symmetric wavefronts.

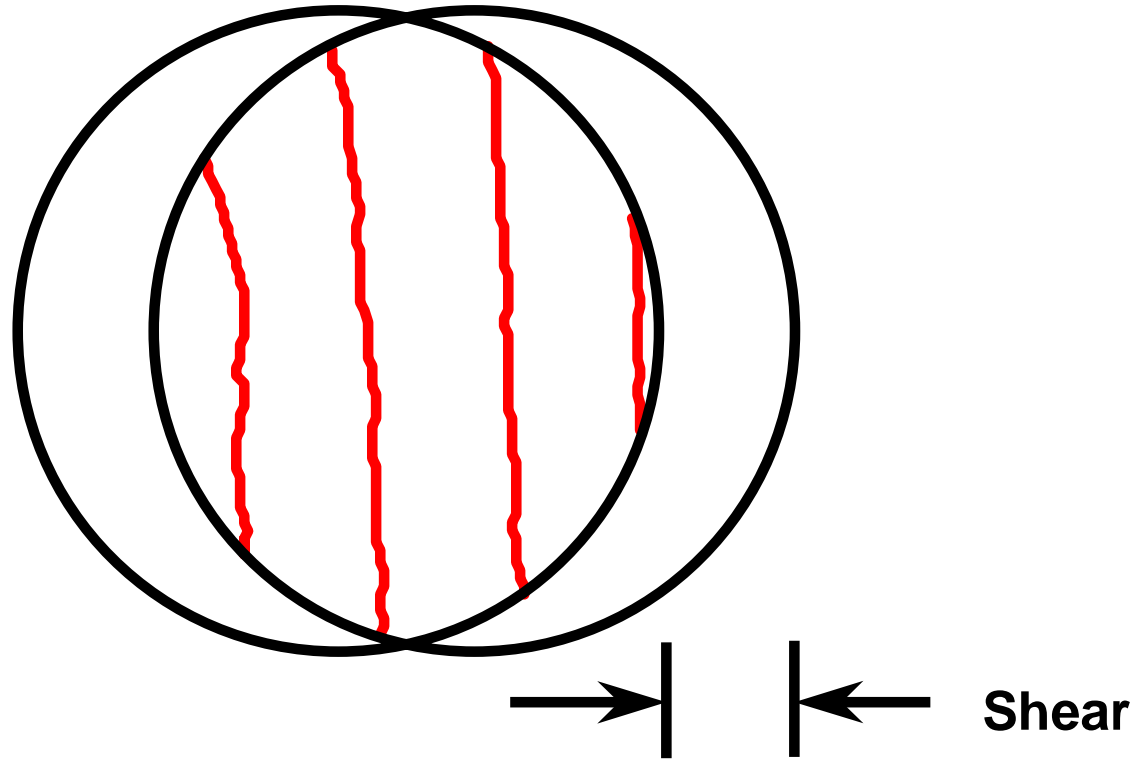
Must know the amount of shear and direction of shear very accurately.

Helps less with wavefronts having larger slopes.

$$\frac{\text{Fringes with LSI}}{\text{Fringes with T - G}} = N \frac{\text{shear distance}}{\text{pupil radius}}$$

N is the power of the aberration, i.e. 4 for fourth-order spherical.

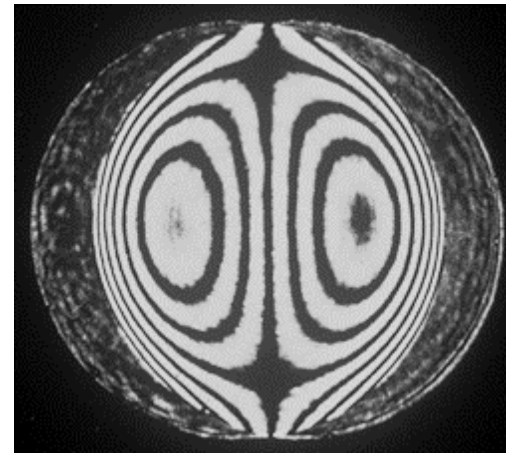
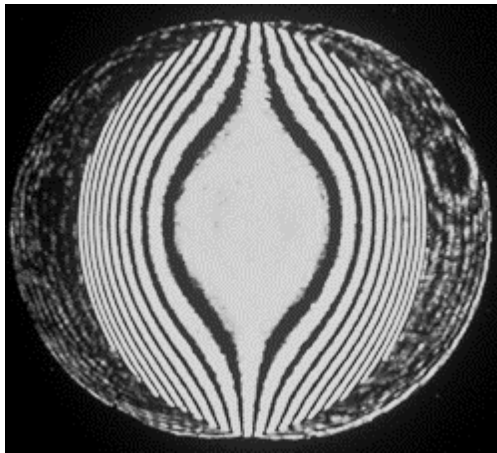
Lateral Shear Interferometry



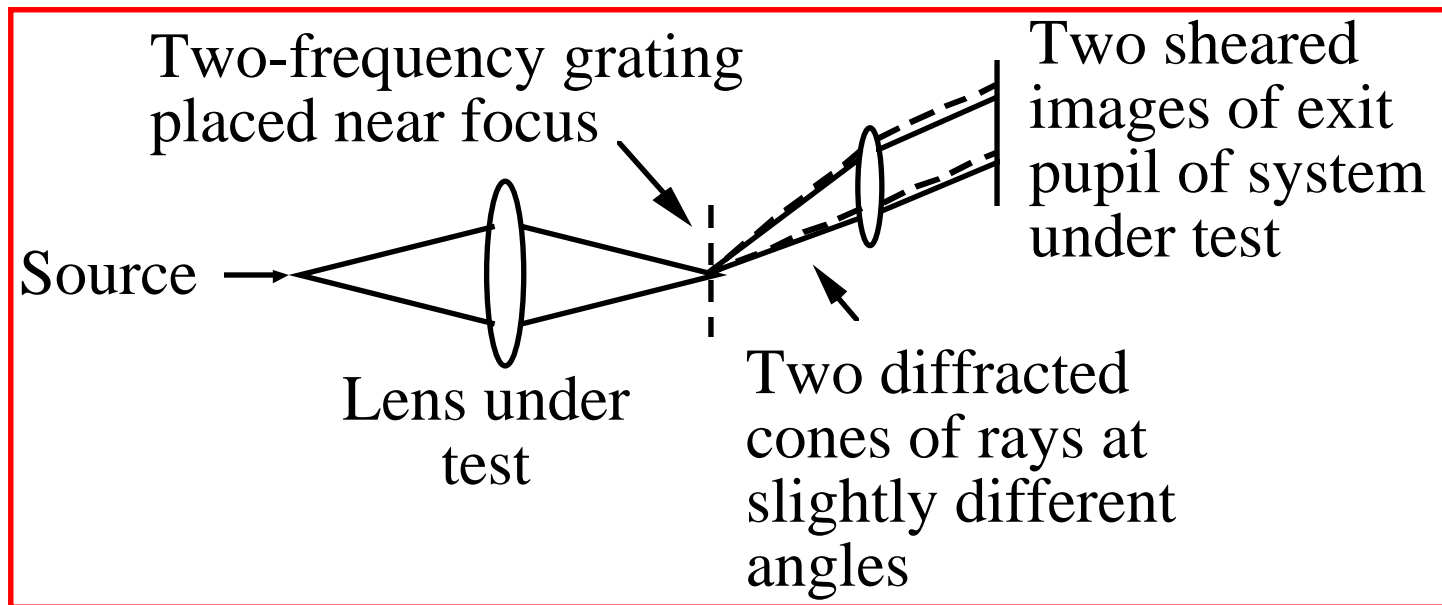
Fringes show loci of constant slope

Sensitivity determined by amount of shear

Typical Lateral Shear Interferograms

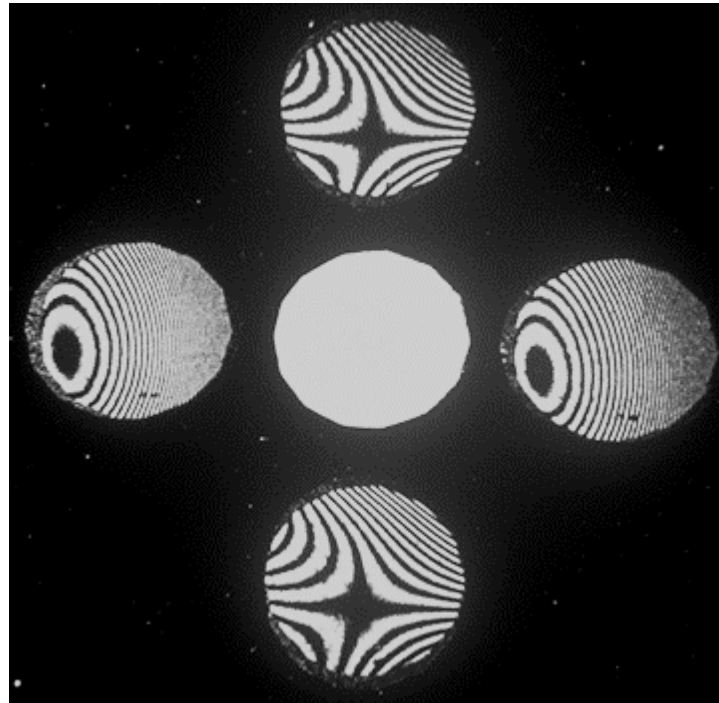


Lateral Shear Interferometer



Measures slope of wavefront, not wavefront shape.

Interferogram Obtained using Grating Lateral Shear Interferometer



9.3.2 Radial shear interferometry

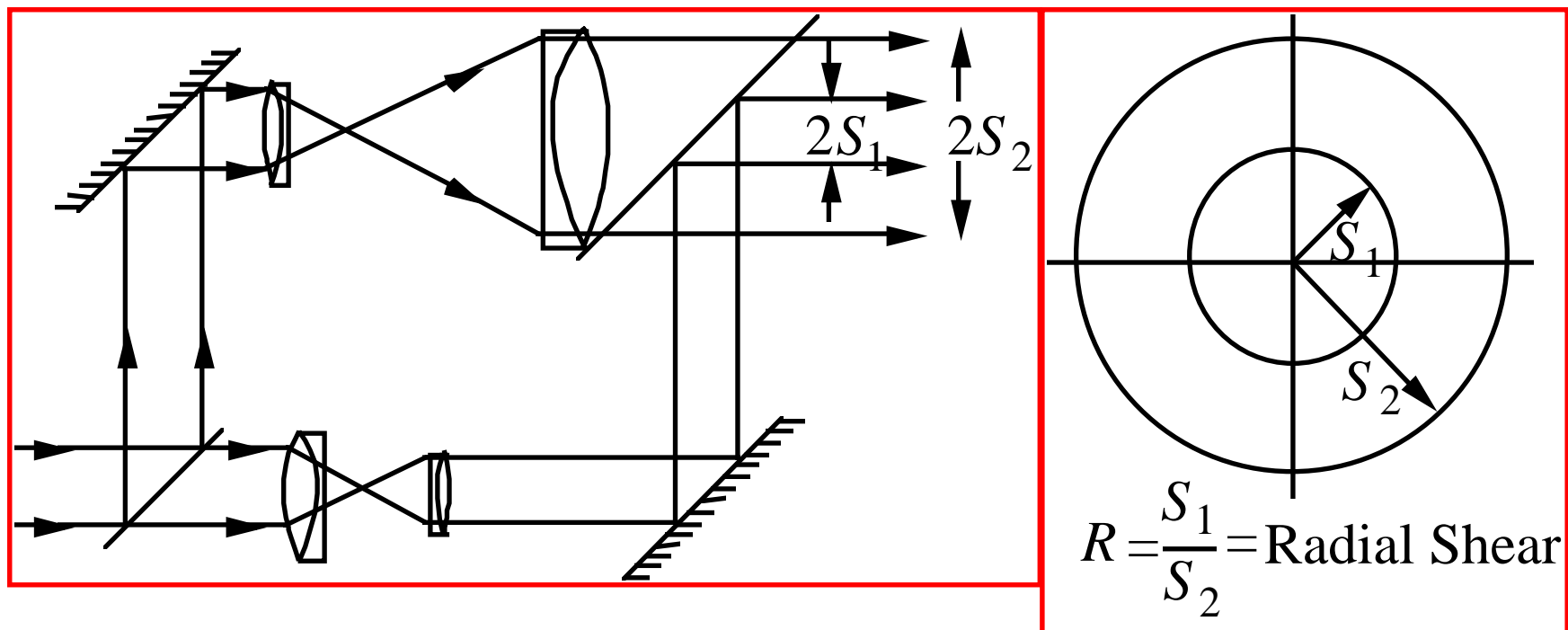
- Advantages

Can vary the sensitivity by varying the amount of radial shear.

- Disadvantages

The shear varies over the pupil with the largest shear at the edge of the pupil, which is generally the location of maximum slope. Thus, we get the least help where we need the most help.

Radial Shear Interferometer



Measures radial slope of wavefront, not wavefront shape.

9.3.3 High-density detector arrays

Theoretically need at least two detectors per fringe if we know nothing about the wavefront we are testing. Due to noise, and the fact that each detector is averaging over a part of a fringe, generally 2.5 or 3 detectors per fringe required. Less than 100% fill factor is desirable, but then more light is required.

If before performing the test we have additional information about the wavefront being tested, such as the surface height to within a quarter wavelength, or that the slope is continuous, it is often possible to perform a measurement using fewer than two detectors per fringe. This will be covered in the next section.

Critical item is to know the system accurately enough so it can be ray traced to determine what the desired asphericity is at the detector plane. Knowing the asphericity at the location of the test object is not enough. We must know the asphericity at the location where the measurement is being performed, i.e. the detector plane. Calibration is probably required.

High-density detector arrays

- **Must have at least two detector elements per fringe.**
- **Interferogram analysis software can remove desired amount of asphericity.**
- **Must ray trace test setup so correct amount of asphericity is known.**

9.3.4 Sub-Nyquist Interferometry

Sub-Nyquist Interferometry

Require fewer than two detector elements per fringe by assuming first and second derivatives of wavefront are continuous

9.3.5 Long-Wavelength Interferometry

Long-Wavelength Interferometry

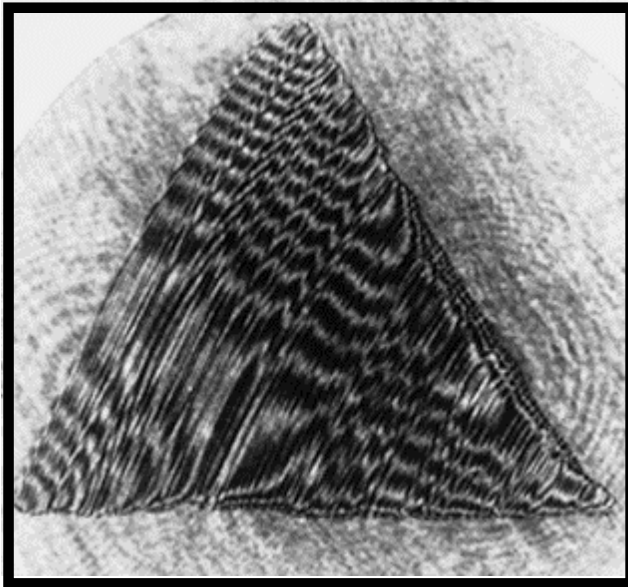
**Reduce number of fringes by
using a long wavelength source
such as a 10.6 micron Carbon
Dioxide laser**

10.6 Micron Source Interferometer

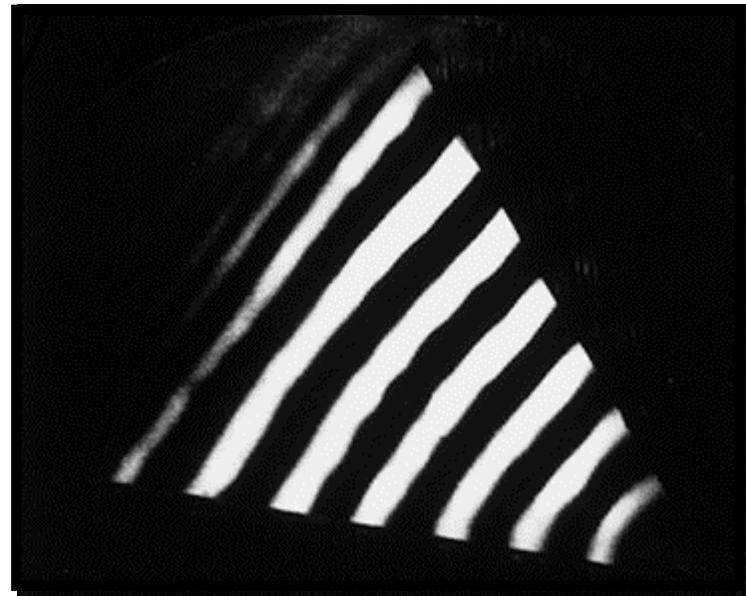
- **Carbon Dioxide Laser**
 - Excellent coherence properties
- **Zinc Selenide or Germanium Optics**
- **Pyroelectric Vidicon Detector**

Conventional interferometry techniques work well.

Reduced Sensitivity Testing



0.633 microns wavelength



10.6 microns wavelength

Testing Rough Surfaces

Assume surface height distribution is Gaussian with standard deviation σ .

The normal probability distribution for the height, h , is

$$p(h) = \frac{1}{(2\pi)^{1/2} \sigma} \exp\left(-\frac{h^2}{2\sigma^2}\right)$$

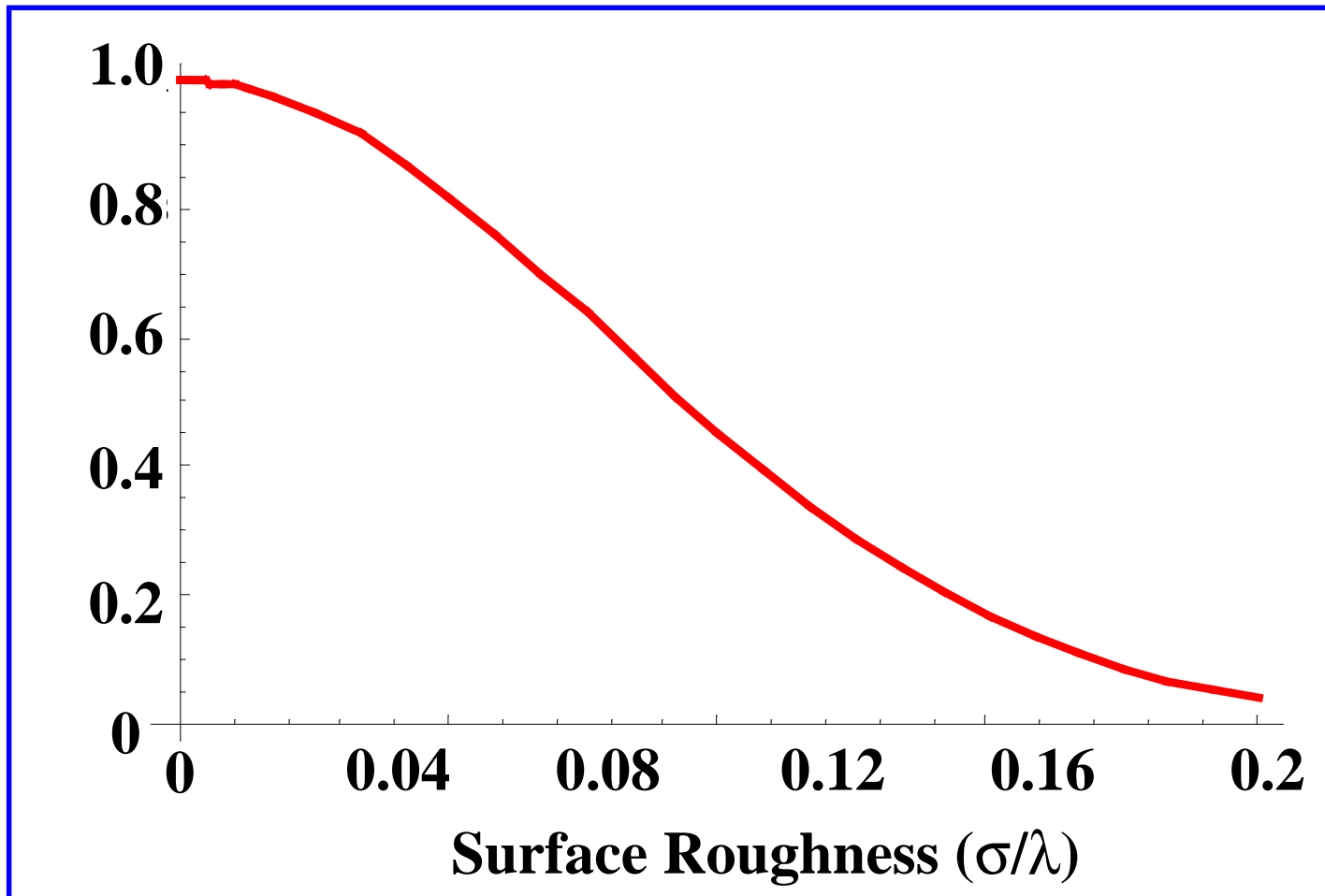
Fringe Contrast Reduction due to Surface Roughness

The fringe contrast reduction due to
surface roughness is

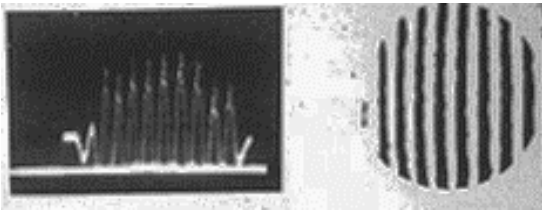
$$C = \exp(-8\pi^2 \sigma^2 / \lambda^2)$$

Reference: Appl. Opt. 11, 1862 (1980).

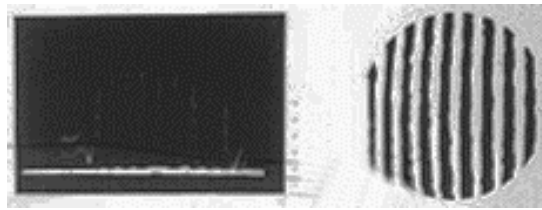
Fringe Contrast versus Surface Roughness - Theory



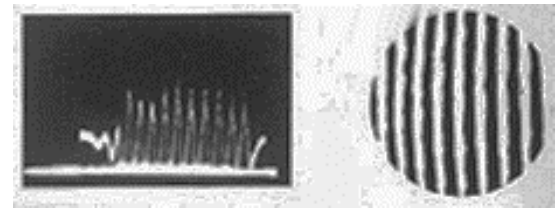
Interferograms Obtained for Different Roughness Surfaces



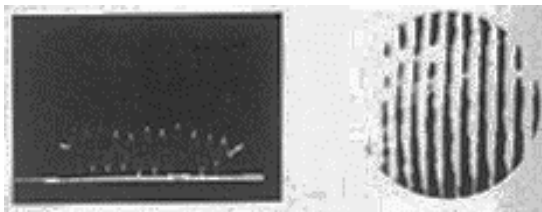
$\sigma = 0 \mu\text{m}, C = 1.0$



$\sigma = 0.32 \mu\text{m}, C = 0.93$



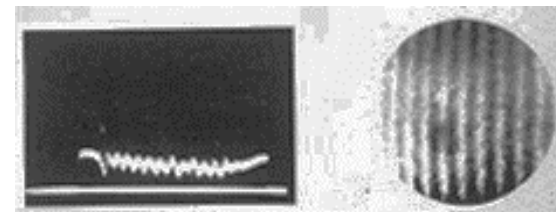
$\sigma = 0.44 \mu\text{m}, C = 0.87$



$\sigma = 0.93 \mu\text{m}, C = 0.54$

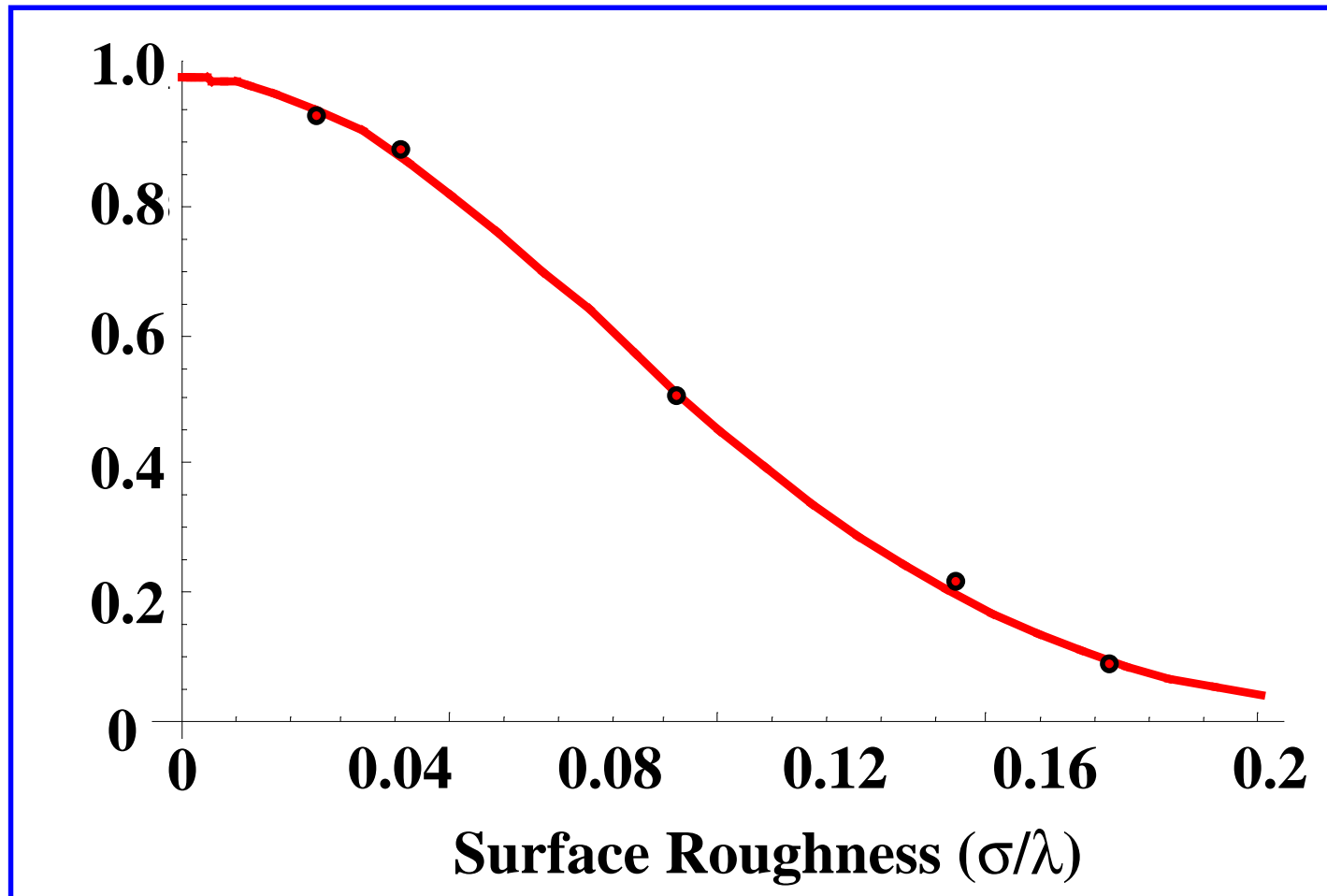


$\sigma = 1.44 \mu\text{m}, C = 0.23$

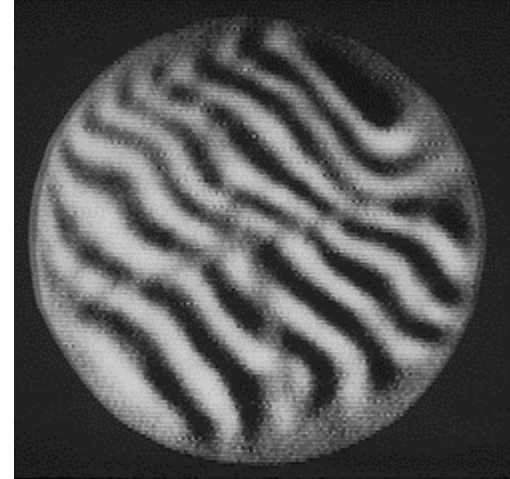
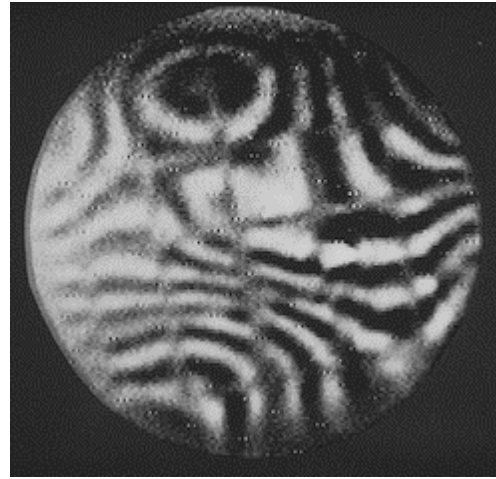
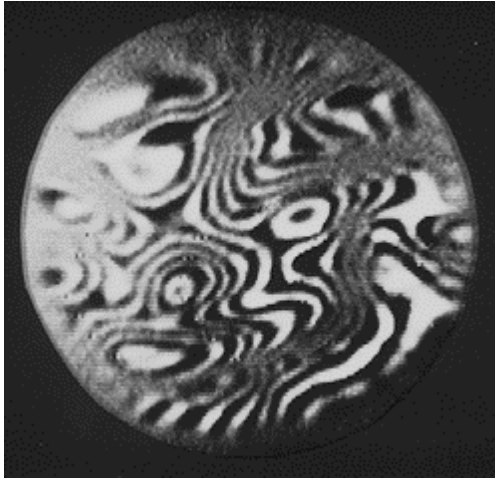


$\sigma = 1.85 \mu\text{m}, C = 0.07$

Fringe Contrast versus Surface Roughness - Theory and Experiment



Infrared Interferograms of Off-Axis Parabolic Mirror



10.6 Micron Wavelength Interferometer



James C. Wyant

9.3.6 Two-Wavelength Holography

Two-Wavelength Holography

We will show that with two-wavelength holography two visible wavelengths can be used to obtain an interferogram having the same sensitivity as a conventional interferogram obtained using a single nonvisible long wavelength.

Let the OPD being measured be $OPD[x, y]$ and the wavelength used to record the hologram be λ_1 . The reference beam is a plane wave with a tilt angle of θ_1 . The normalized irradiance used in recording the hologram is then given by

$$\text{irradiance}[\mathbf{x}, \mathbf{y}] = \text{Abs} \left[e^{i \frac{2\pi}{\lambda_1} OPD[\mathbf{x}, \mathbf{y}]} + e^{i \frac{2\pi}{\lambda_1} \mathbf{x} \sin[\theta_1]} \right]^2 = 1 + 1 + e^{i \frac{2\pi}{\lambda_1} (OPD[\mathbf{x}, \mathbf{y}] - \mathbf{x} \sin[\theta_1])} + e^{-i \frac{2\pi}{\lambda_1} (OPD[\mathbf{x}, \mathbf{y}] - \mathbf{x} \sin[\theta_1])}$$

We will make the usual assumption that the amplitude transmission of the processed hologram is proportional to the irradiance used to expose the hologram.

$$\mathbf{t}[\mathbf{x}, \mathbf{y}] = \mathbf{t}_b + \beta (\text{irradiance}[\mathbf{x}, \mathbf{y}])$$

We will change the wavelength of the source from λ_1 to λ_2 and the angle of the reference beam from θ_1 to θ_2 and illuminate the processed hologram with the object beam and the reference beam.

$$\text{illumination} = e^{i \frac{2\pi}{\lambda_2} OPD[\mathbf{x}, \mathbf{y}]} + e^{i \frac{2\pi}{\lambda_2} \mathbf{x} \sin[\theta_2]}$$

The two beams in the reconstruction of interest are the zero order from the test beam and the diffracted order from the reference beam. These two beams will be proportional to

$$2 e^{i \frac{2\pi}{\lambda_2} OPD[\mathbf{x}, \mathbf{y}]} + e^{i \frac{2\pi}{\lambda_1} OPD[\mathbf{x}, \mathbf{y}]} e^{i 2\pi \left(\frac{\mathbf{x} \sin[\theta_2]}{\lambda_2} - \frac{\mathbf{x} \sin[\theta_1]}{\lambda_1} \right)}$$

As long as angle between the test and reference beams are large enough the other orders will separate from these two beams and the resulting interference pattern will be given by the interference of these two beams.

$$\mathbf{i} = \mathbf{a} + \mathbf{b} \text{Cos} \left[2\pi OPD[\mathbf{x}, \mathbf{y}] \left(\frac{1}{\lambda_1} - \frac{1}{\lambda_2} \right) + 2\pi \mathbf{x} \left(\frac{\sin[\theta_2]}{\lambda_2} - \frac{\sin[\theta_1]}{\lambda_1} \right) \right]$$

We can write

$$2\pi \left(\frac{1}{\lambda_1} - \frac{1}{\lambda_2} \right) OPD[\mathbf{x}, \mathbf{y}] = \frac{2\pi}{\lambda_{\text{eq}}} OPD[\mathbf{x}, \mathbf{y}], \text{ where}$$

$$\frac{1}{\lambda_{\text{eq}}} = \left(\frac{1}{\lambda_1} - \frac{1}{\lambda_2} \right) \quad \text{or} \quad \lambda_{\text{eq}} = \frac{\lambda_1 \lambda_2}{\text{Abs}[\lambda_1 - \lambda_2]}$$

Double exposure techniques will work as well as the real-time technique described above, although the real-time technique is generally preferred because the tilt in the final interferogram can be easily changed by varying θ_2 and it is easy to apply phase-shifting techniques.

Since the two-wavelength holography technique involves finding the difference between two interferograms formed at the two different wavelengths any difference between the two interferograms introduced by chromatic aberration or disturbances such as air turbulence will introduce errors. To make

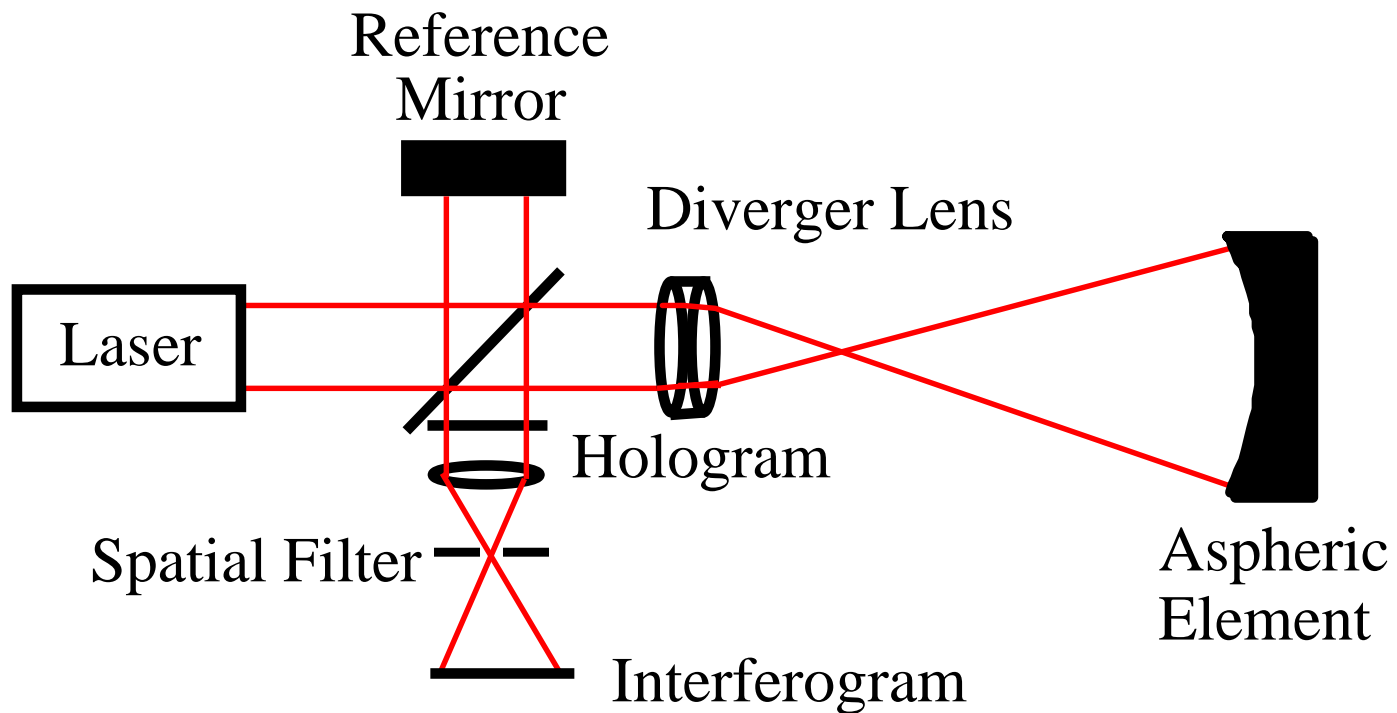
matters worse, the differences will be scaled by the equivalent wavelength. That is, one fringe error between the two interferograms corresponds to an error of λ_{eq} , not λ_1 or λ_2 .

Two-Wavelength Holography

- **Means of using visible light to perform interferometric test having sensitivity of test performed using a long-wavelength nonvisible source**
- **Record hologram at wavelength λ_1**
- **Reconstruct hologram at wavelength λ_2 .**
- **Interferogram same as would be obtained using wavelength**

$$\lambda_{\text{eq}} = \frac{\lambda_1 \lambda_2}{|\lambda_1 - \lambda_2|}$$

Two Wavelength Holography Interferometer

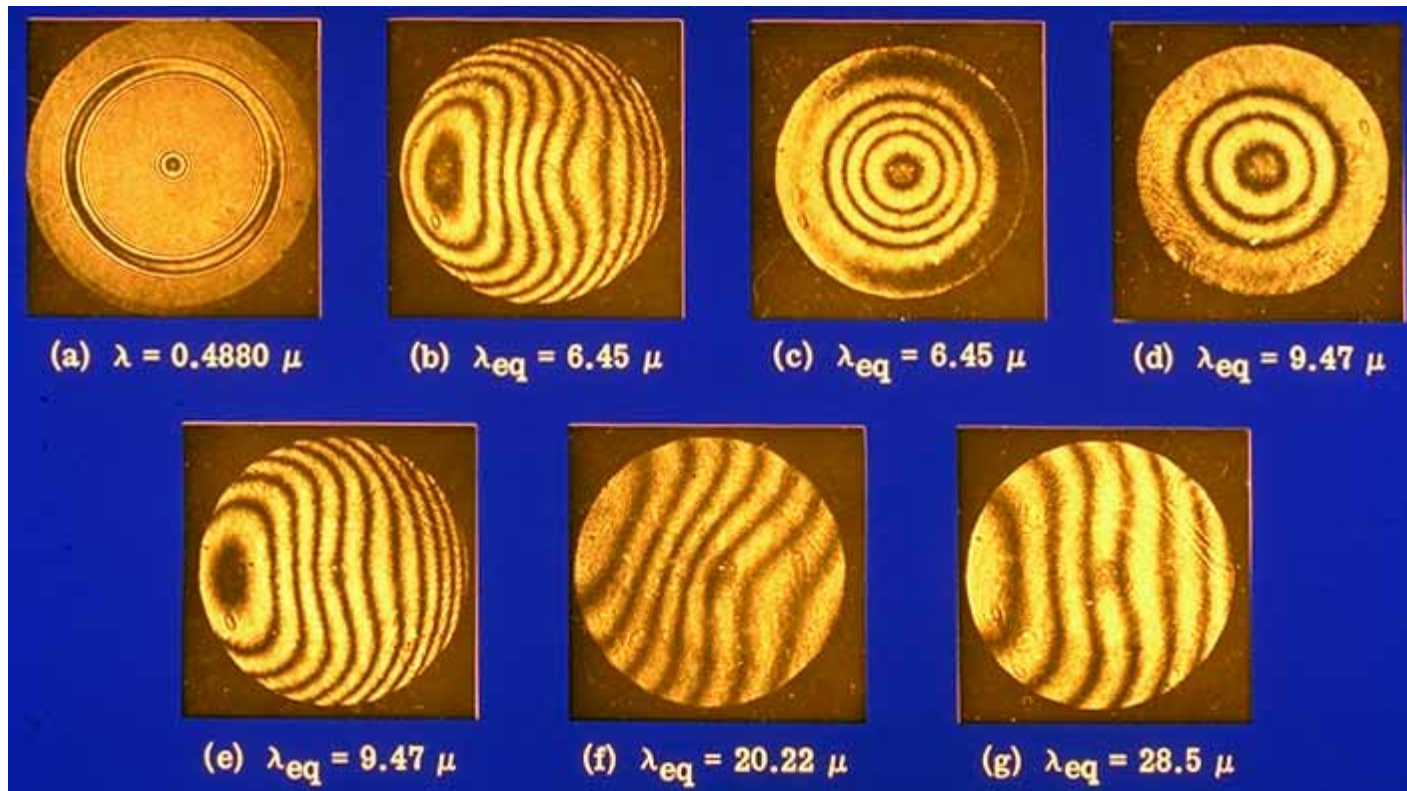


Possible Equivalent Wavelengths obtained with Argon and HeNe Lasers

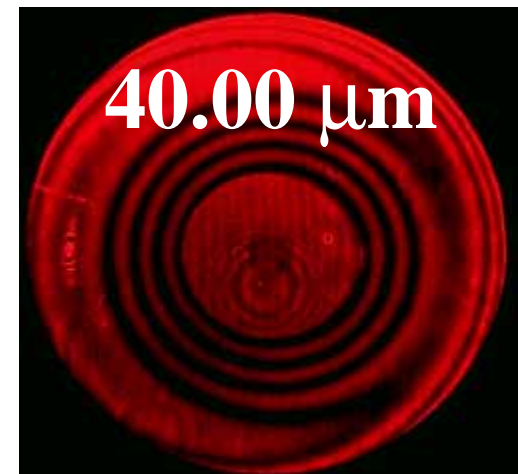
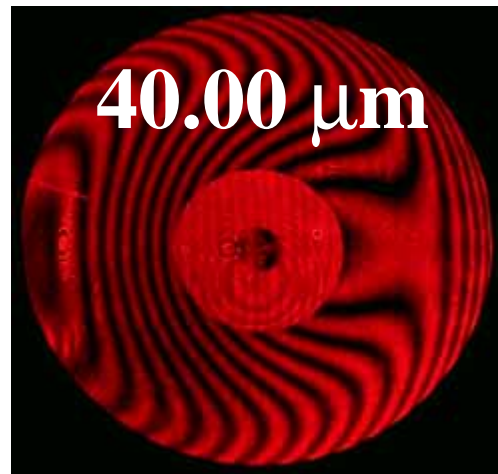
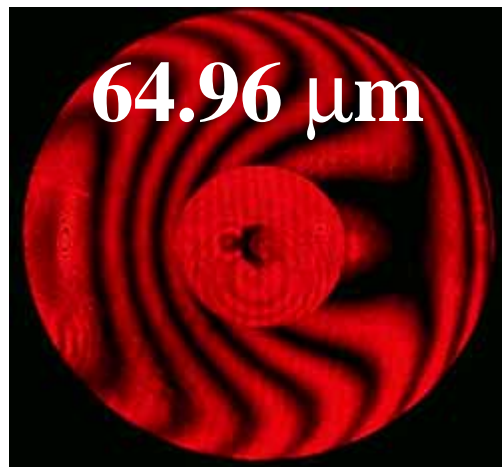
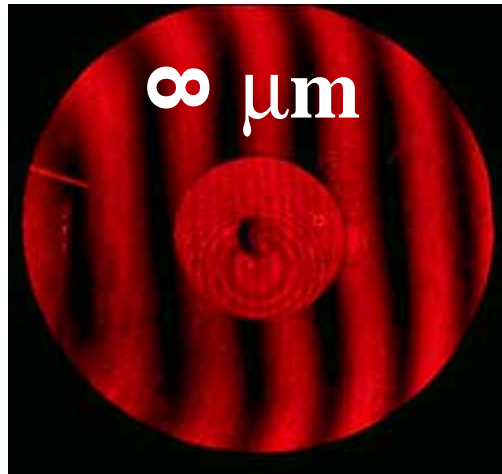
$\lambda_2 \backslash \lambda_1$	0.4579	0.4765	0.4880	0.4965	0.5017	0.5145	0.6328
0.4579	-	11.73	7.42	5.89	5.24	4.16	1.66
0.4765	11.73	-	20.22	11.83	9.49	6.45	1.93
0.4880	7.42	20.22	-	28.50	17.87	9.47	2.13
0.4965	5.89	11.83	28.50	-	47.90	14.19	2.31
0.5017	5.24	9.49	17.87	47.90	-	20.17	2.42
0.5145	4.16	6.45	9.47	14.19	20.17	-	2.75
0.6328	1.66	1.93	2.13	2.31	2.42	2.75	-

$$\lambda_{\text{eq}} = \frac{\lambda_1 \lambda_2}{|\lambda_1 - \lambda_2|}$$

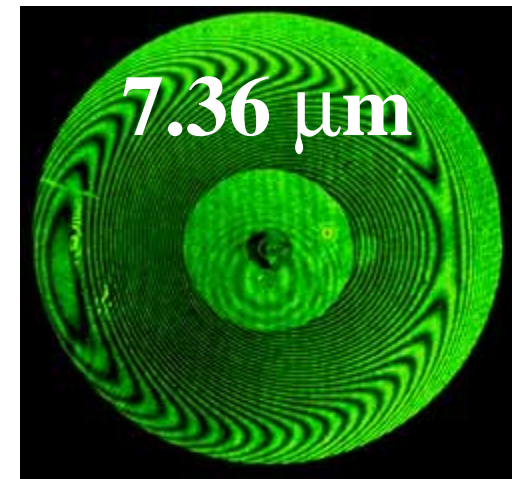
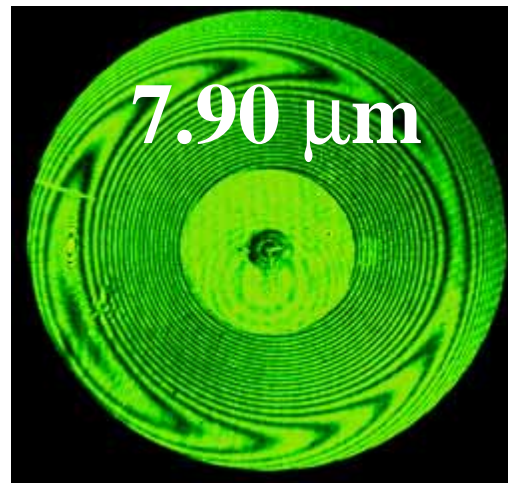
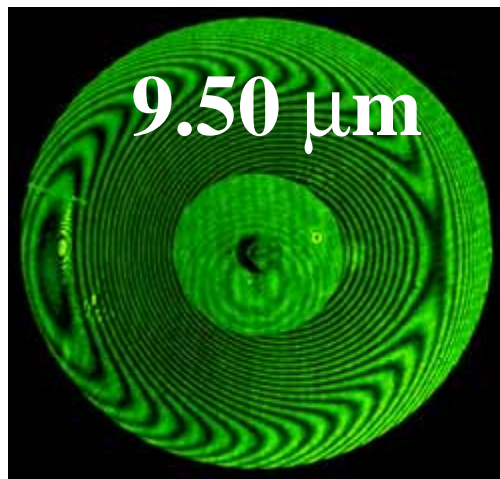
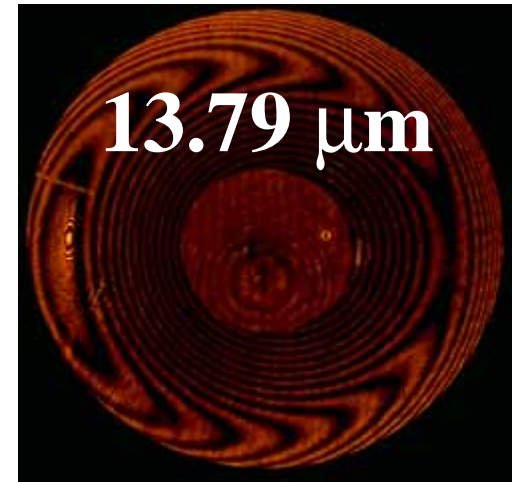
Two Wavelength Holography Interferograms



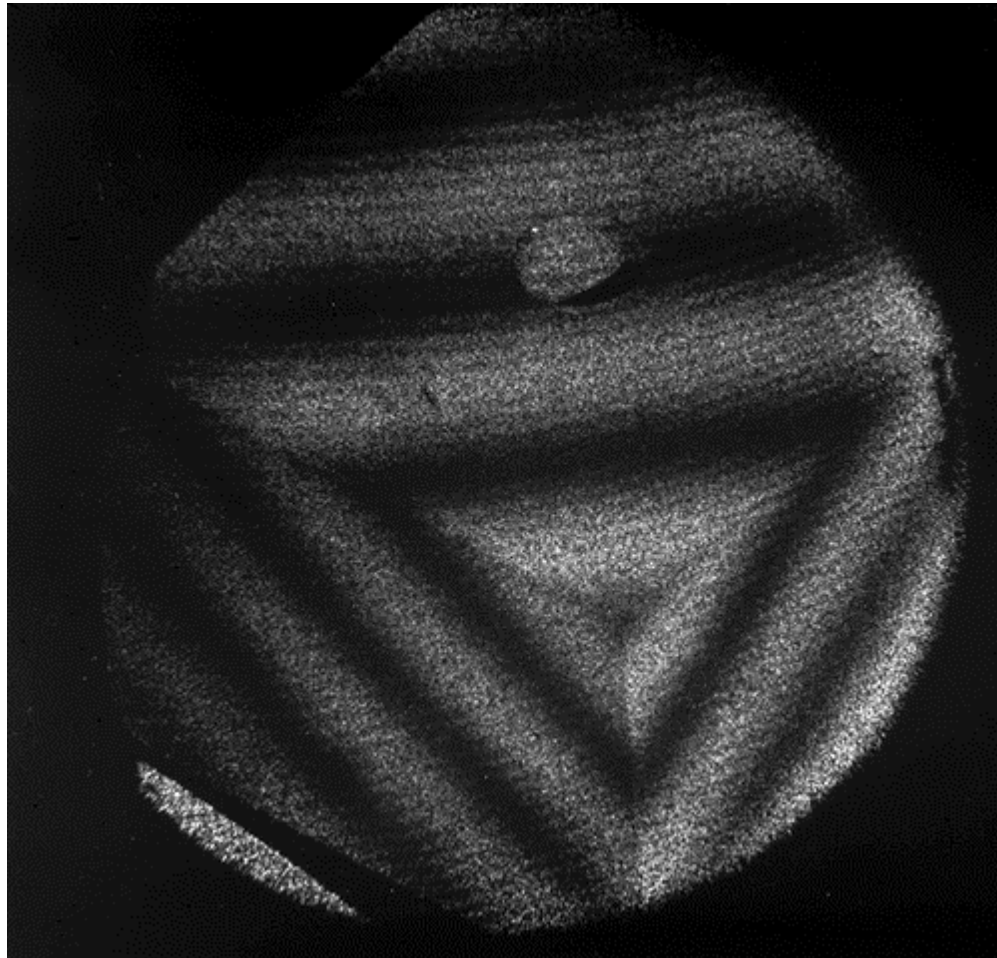
Dye Laser Interferograms I



Dye Laser Interferograms II

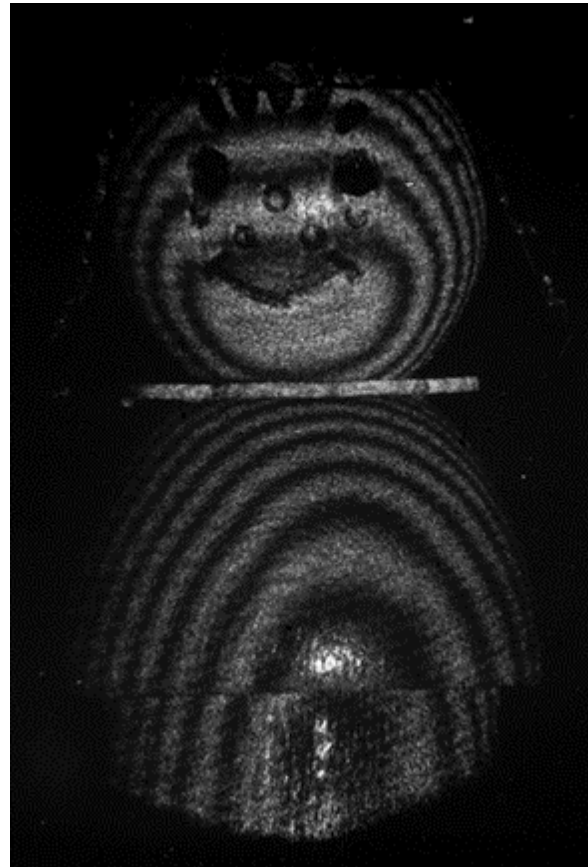


TWH Test of Aluminum Block



$\lambda_{eq} = 10 \text{ mm}$

TWH Test of Seaseme Street Character



$$\lambda_{eq} = 2 \text{ mm}$$

9.3.7 Two-Wavelength Interferometry

Two-Wavelength Interferometry

Perform measurement at two wavelengths, λ_1 and λ_2 .

Computer calculates difference between two measurements.

Wavefront sufficiently sampled if there would be at least two detector elements per fringe for a wavelength of

$$\lambda_{\text{eq}} = \frac{\lambda_1 \lambda_2}{|\lambda_1 - \lambda_2|}$$

9.3.8 Moiré Interferometry

Moiré Interferometry (Projected Fringe Contouring)

Ref: A. MacGovern, Appl. Opt. 11, 2972 (1972).

If parallel, equispaced planes or fringes are projected onto a non-planar surface and the surface is viewed at an angle different from that at which the fringes are projected, curved fringes are seen. The fringes are contour lines of the surface relative to a plane surface. The contour interval depends upon the spacing of the fringes projected onto the surface and the projection angle and viewing angle.

Let the surface to be tested be described by the function

$$z = f[x, y]$$

Let the loci of fringes projected on a surface be given by

$$y = z \tan[\alpha] + n d$$

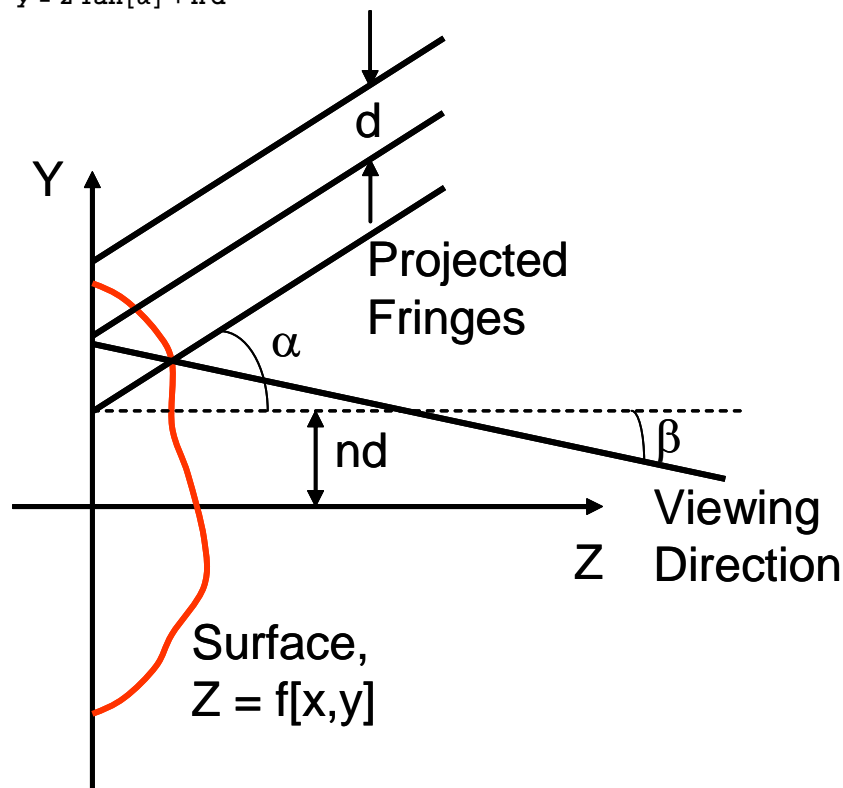


Figure 1. Intersection of projected fringes on surface.

Then

$$y = f[x, y] \tan[\alpha] + n d$$

If the surface is viewed at angle β , then it will appear as though the fringe is intersecting the surface at

$$y = f[x, y] \tan[\alpha] + n d + f[x, y] \tan[\beta]$$

or

$$y = f[x, y] (\tan[\alpha] + \tan[\beta]) + n d$$

If this surface were tested in a Twyman-Green using a wavelength λ and a plane reference wavefront tilted an angle γ a bright fringe would be obtained whenever

$$2 f[x, y] - y \sin[\gamma] = -n \lambda$$

or

$$y = \frac{2 f[x, y]}{\sin[\gamma]} + \frac{n \lambda}{\sin[\gamma]}$$

Comparing the equations for the projected lines and the Twyman-Green interferogram we see

$$\frac{2}{\sin[\gamma]} = \tan[\alpha] + \tan[\beta]$$

and

$$\frac{n \lambda_{\text{eq}}}{\sin[\gamma]} = n d \quad \text{or} \quad \frac{2}{\sin[\gamma]} = \frac{2 d}{\lambda_{\text{eq}}}$$

Thus we can write

$$\lambda_{\text{eq}} = \frac{2 d}{\tan[\alpha] + \tan[\beta]}$$

An image of the intersection of the projected fringes with the surface being tested looks like a Twyman-Green interferogram of the surface where the equivalent wavelength is given by $\lambda_{\text{eq}} = \frac{2d}{\tan[\alpha] + \tan[\beta]}$. If we form a moiré of this image with a straight line pattern the amount of tilt in the "equivalent" interferogram is changed.

The contour interval is $\frac{\lambda_{\text{eq}}}{2}$ or

$$\text{contourInterval} = \frac{\lambda_{\text{eq}}}{2} = \frac{d}{\tan[\alpha] + \tan[\beta]}$$

12.5. MOIRÉ INTERFEROMETRY

Moiré interferometry, which can be regarded as a form of holographic interferometry, is a complement to conventional holographic interferometry, especially for testing optics to be used at long wavelengths. Although TWH can be used to contour surfaces at any longer-than-visible wavelength, visible interferometric environmental conditions are required. Moiré interferometry can be used to contour surfaces at any wavelength longer than $10\ \mu\text{m}$ (with difficulty) or $100\ \mu\text{m}$ with reduced environmental requirements and no intermediate photographic recording setup. For non-destructive testing, holographic interferometry has a precision of a small fraction of a micrometer and is useful over a deformation amplitude of a few micrometers, whereas moiré interferometry has a precision ranging from $10\text{-}100\ \mu\text{m}$ to millimeters, with a correspondingly increased useful range of deformation amplitude.

125.1. Basic Principles

Although moiré techniques have been used for many years, only recently has the full potential of moiré interferometry been realized (Brooks and Heflinger 1969, Takaski, 1970, 1973, MacGovern 1972, Benoit et al. 1975). If parallel equispaced planes or fringes are projected onto a nonplanar

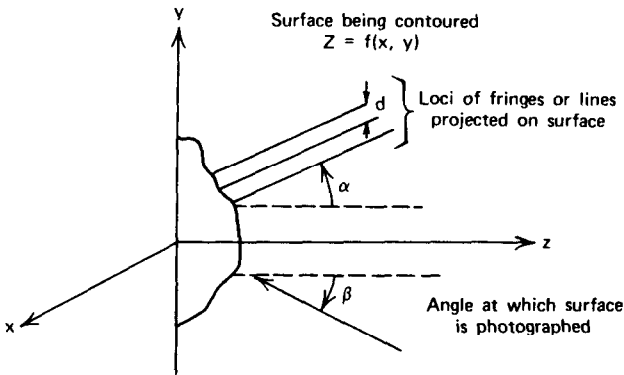


Figure 12.14. Fringes projected on surface $Z = f(x, y)$ at angle α and viewed at angle β .

surface and the surface is viewed at an angle different from that at which the fringes are projected, curved fringes are seen. It can be shown that a photograph of these fringes is equivalent to a hologram made of the surface using a long wavelength light source (MacGovern 1972). If a surface described by the function $Z=f(x,y)$ is illuminated and viewed as shown in Fig. 12.14, a photograph of the projected fringes shows contour lines of the surface relative to a plane surface, where the contour interval C is given by

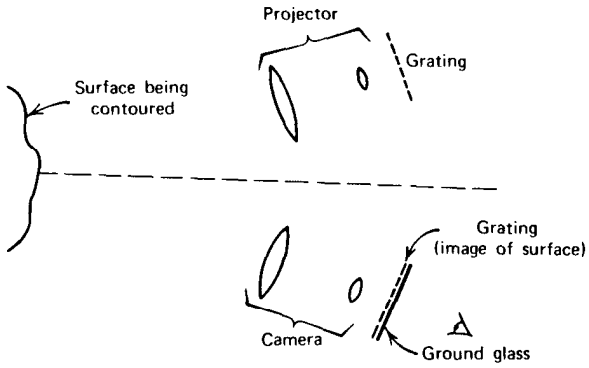
$$C = \frac{d}{\tan \alpha + \tan \beta} \tag{12.7}$$

The sign convention used for the angles is shown in the figure. The moire pattern of the photograph of the projected fringes, as compared with a straight line pattern, is equivalent to changing the tilt of the reference surface. The moiré pattern of two photographs of projected fringes for two different objects gives the difference between the two objects, for example, a master optical surface and another supposedly identical optical surface. Likewise, deformation measurements can be made.

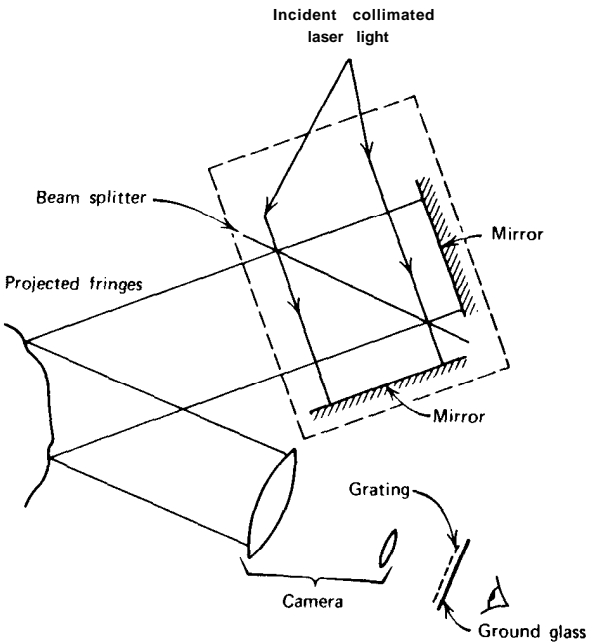
12.52. Experimental Setups

Several experimental setups can be used to perform moire interferometry, of which three are illustrated in Figs. 12.15 to 12.17.

In Fig. 12.15a a grating is projected onto the surface being contoured. There is no requirement that the light be coherent or even monochromatic. Both the camera and the grating projector should be telecentric systems so that the angles of projection and view are well defined. The surface being



(a)



(b)

Figure 12.15. Experimental setups for moiré interferometry. (a) Projecting grating on surface. (b) Projecting fringes on surface.

contoured is imaged onto a grating so as to select the desired tilt of the reference plane. If ground glass is placed next to the second grating, the moiré pattern can be viewed directly. The moiré pattern can be photographed by replacing the ground glass with a sheet of film. This technique has the disadvantage that the relatively high frequency fringes must be transferred through an optical system with attendant loss of contrast. In addition, the projector has a limited depth of focus.

To meet this objection, the grating projector can be replaced with an interferometer, as shown in Fig. 12.15b. In this case a coherent laser beam is used, and a beam splitter with one mirror slightly tilted produces nonlocalized interference fringes, which fall on the surface to be contoured. This method has the advantage that, since the lines projected on the surface are nonlocalized fringes resulting from the interference of two collimated beams, there are no depth-of-focus problems in the projection system.

The higher frequency (carrier frequency) will be displayed on the final photograph unless some effort is made to avoid it. One technique to eliminate the carrier frequency is to use spatial filtering, as illustrated in Fig. 12.16. A second technique is to raise the carrier frequency above the resolution limit of the film. For instance, Polaroid film has a resolution limit of 22 to 28 line pairs per millimeter; since the moiré pattern is created before the film plane, only the relatively coarse moiré will be recorded if the carrier frequency exceeds about 22 line pairs per millimeter.

A third possible setup is shown in Fig. 12.17. In this case the same grating is used for both projecting and viewing. This setup has the advantage that the camera does not have to resolve the higher frequency grating lines, and must be capable of resolving only the moiré. This, in principle, yields a higher contrast moiré pattern. Another advantage is that the grating may be freely translated (but not rotated) in its plane without changing the perceived moiré pattern. If the grating is slowly moved during the recording exposure, it will not appear on the photograph; only the stationary moiré pattern will be recorded. The perceived sensitivity (fringes per unit deformation) may be varied easily by rotating the grating; it goes to zero when the grating lines lie parallel to the light source-camera

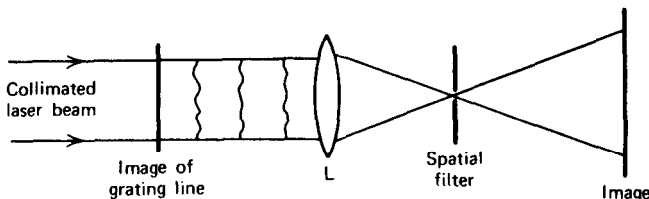


Figure 12.16. Use of spatial filtering to eliminate carrier frequency.

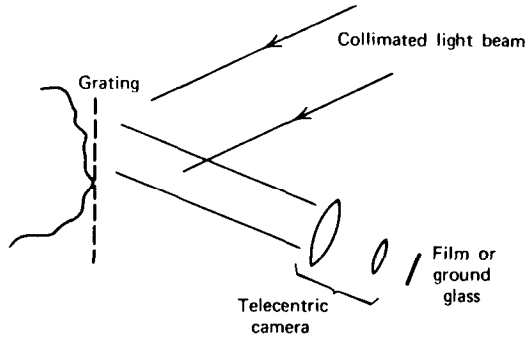


Figure 12.17. Use of single grating for projection and viewing.

plane. Finally, the contouring may be performed with white light, where projector and camera are telecentric and have a large relative aperture. This technique has the disadvantage that the grating must be reasonably near the surface being contoured. This requirement is relaxed, however, as the light source becomes better collimated, the camera lens goes to larger f numbers, and the carrier frequency decreases.

12.53. Experimental Results

Figure 12.18 shows results obtained testing a spherical surface in the setup shown in Fig. 12.17. The equivalent wavelength in this instance was $200\ \mu\text{m}$. As stated above, moiré interferometry is definitely a complement to conventional holography and should be of particular use in testing components for longer wavelength optical systems.

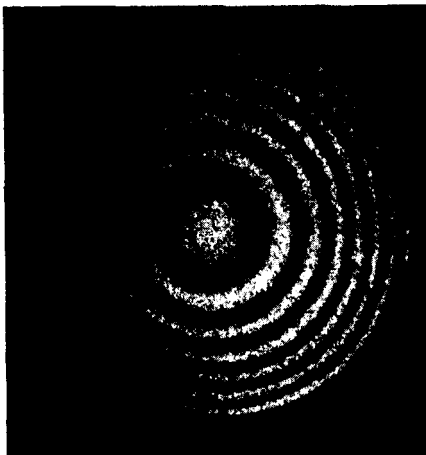
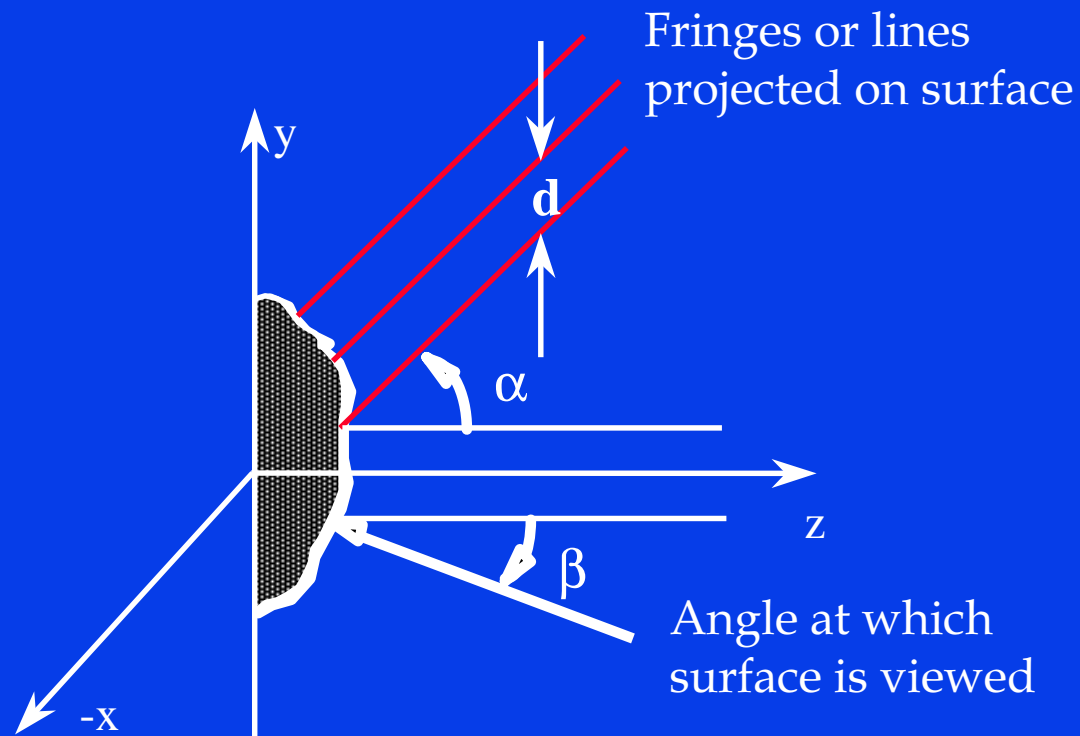


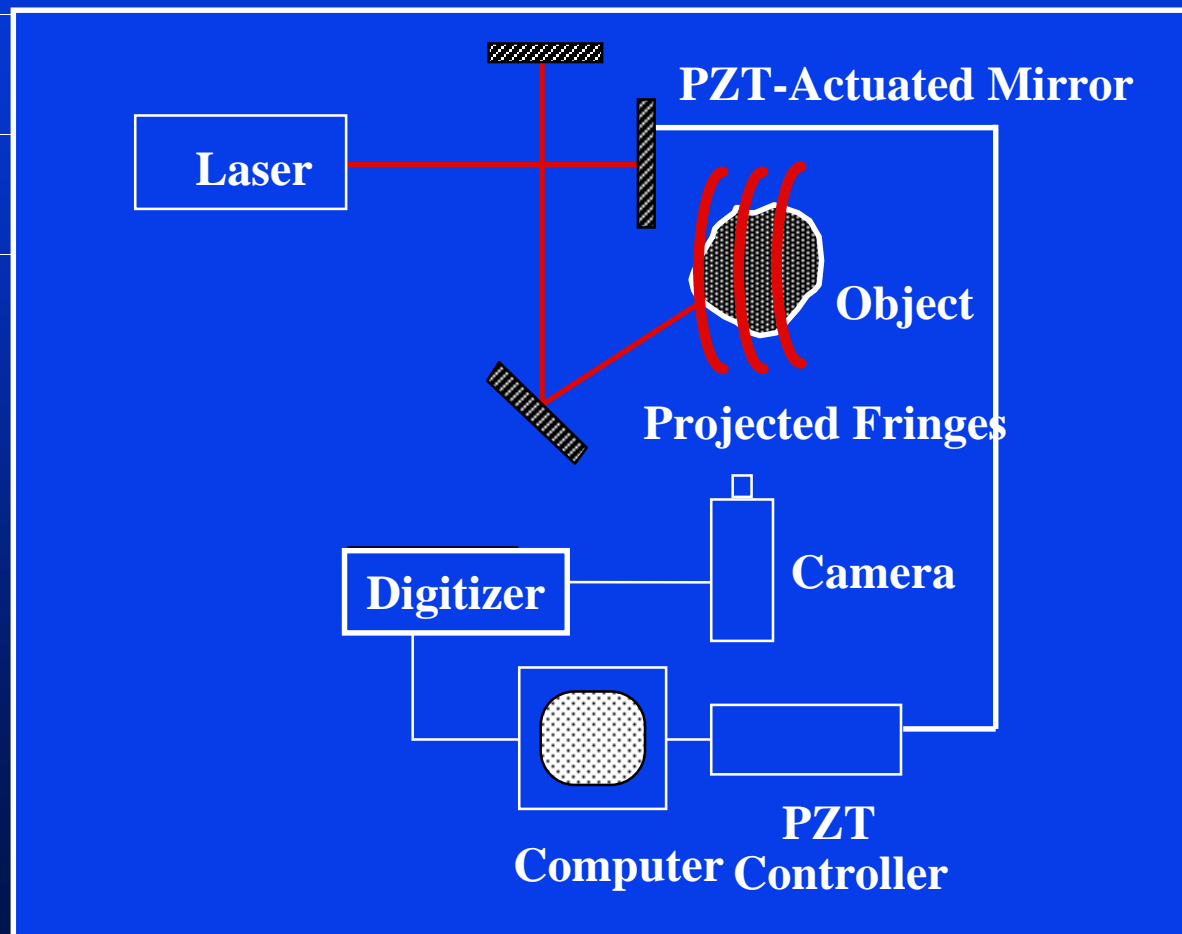
Figure 12.18. Moiré interferogram obtained when testing a spherical mirror ($\lambda_{\text{eq}} = 200\ \mu\text{m}$).

Projected Fringe Contouring

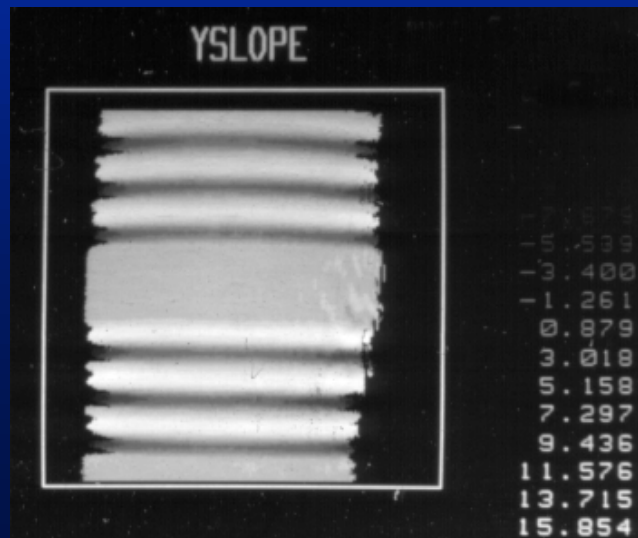
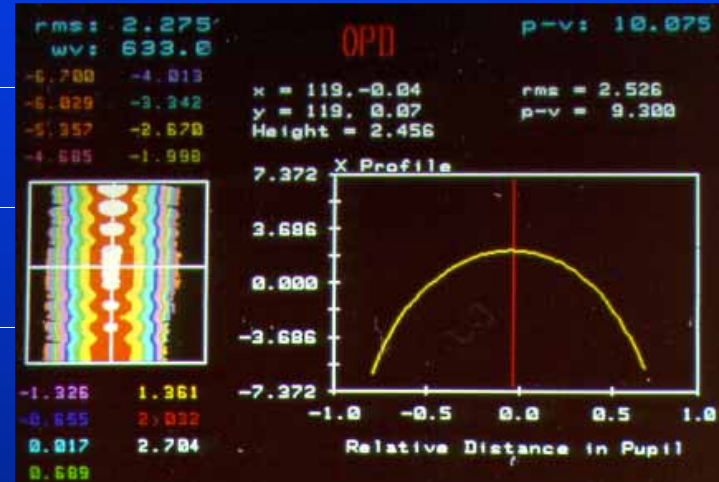
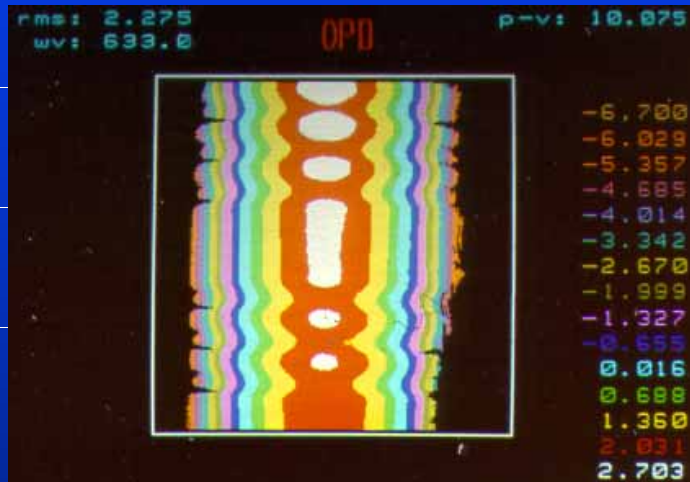


$$\lambda_{eq} = \frac{2d}{\tan\alpha + \tan\beta}$$

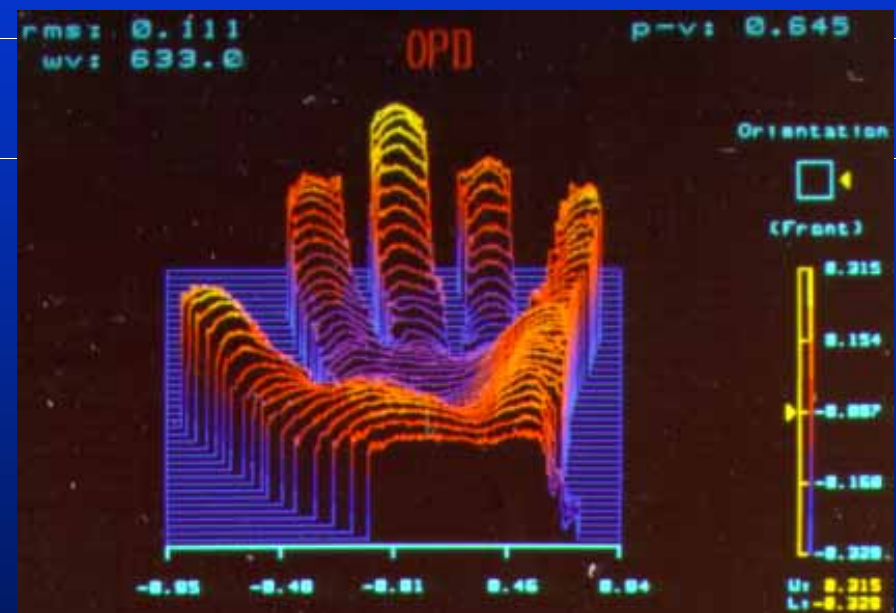
Projected Fringe Contouring Setup



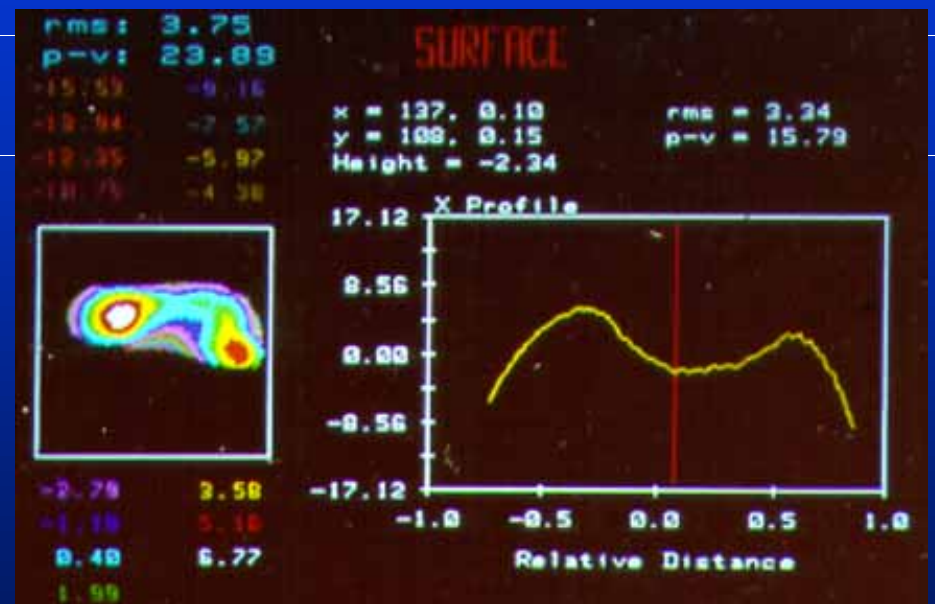
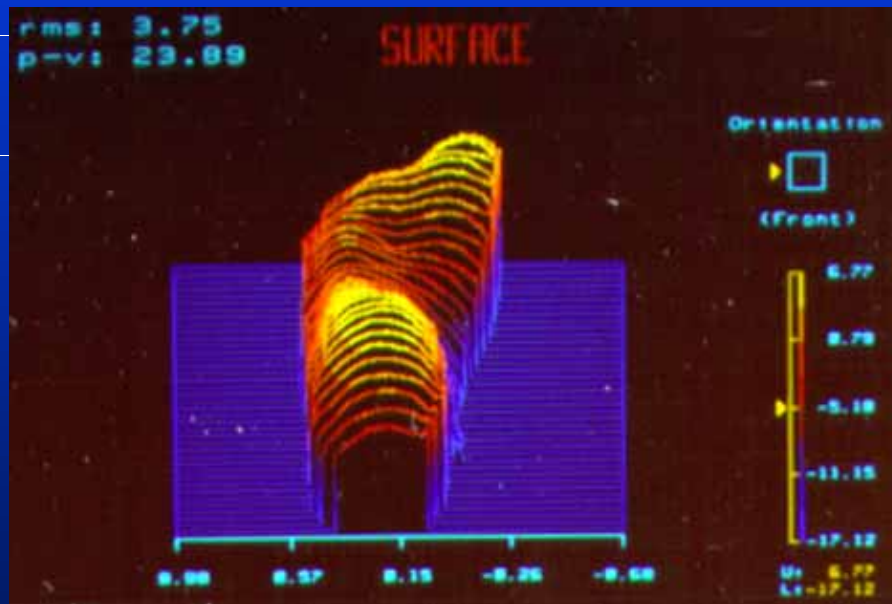
Can



Hand



Foot



Foot Scanner



Lens Analysis Software

- **Must know precisely how optics in test setup change aspheric wavefront.**
- **Must know effects of misalignments, so errors due to misalignments can be removed.**

Basic Limitations of Aspheric Testing

- **Must get light back into the interferometer**
- **Must be able to resolve the fringes**
- **Must know precisely the optical test setup**

This is the most serious problem